Compressed Sensing for Electron Tomography

Matthew Guay

University of Maryland, College Park
Department of Mathematics

Norbert Wiener Center
for Harmonic Analysis and Applications

February 10, 2015

Outline I

1. Introduction
2. Radon transforms and compressed sensing
3. Sparsity across application domains
4. Experimental results

1 Introduction

2 Radon transforms and compressed sensing

3 Sparsity across application domains

4 Experimental results

Tomography

- Tomography - Producing a 3D reconstruction of an object by measuring changes in penetrating waves (or particles) which are sent through it. Many modalities, depending on wave type:

CT - X-rays	MRI - Radio waves
ET - Electrons	PET - Electron-positron annihilation

- Electron tomography (ET) - 3D imaging using electron beams via a transmission electron microscope (TEM) or scanning transmission electron microscope (STEM).

Our ET data

- Our NIH collaborators have provided STEM images of heavy metal-stained sections of cells, rotated incrementally about a fixed axis.
- Each image is a projection of the rotated object, a sequence of images indexed by rotation angle is a tilt series.
- Bright field STEM imaging: detectors measure electron beam attenuation through the object.
- Projections show intensity amplitude contrast due to the scattering of electrons by dense regions within the object.

From tomography to Radon transforms

- A beam of n_0 electrons travels along line L through the object at each detector location, which counts the n electrons passing through undeviated.
- The ratio $\frac{n}{n_0}$ can be related to line integrals of an electron density function $f(\boldsymbol{x}) : \mathbb{R}^3 \to \mathbb{R}$ via the Beer-Lambert law:

$$\log\left(\frac{n}{n_0}\right) \propto \int_L f(\boldsymbol{x})\,|d\boldsymbol{x}| \tag{1}$$

- The function f forms the tomogram recovered from the projection data.

From tomography to Radon transforms

- **Radon transform** - for $f : \mathbb{R}^2 \to \mathbb{R}$ and any line $L \subseteq \mathbb{R}^2$,

$$Rf(L) = \int_L f(\boldsymbol{x})\,|d\boldsymbol{x}|. \tag{2}$$

- This space of lines can be parametrized by a normal angle θ and a distance coordinate s:

$$Rf(\theta, s) = \int_{-\infty}^{\infty} f((t\sin\theta + s\cos\theta), (-t\cos\theta + s\sin\theta))\,dt.$$

From tomography to Radon transforms

- Parallel beam tomography used in ET decomposes 3D reconstruction into multiple independent 2D reconstruction problems.
- For each plane normal to the rotation axis, tomographic measurements provide samples $\{Rf(\theta_i, s_j)\}_{i \in I, j \in J}$ for some finite sets I, J.
- Measurement limitations make tomogram recovery an ill-posed operator inversion problem, either of R or the 2D Fourier transform due to the Fourier-slice theorem.

The Fourier-slice theorem

- Fixing θ, the 1D Fourier transform of $Rf(\theta, s)$ in s can be related to the 2D Fourier transform of f.
- **Fourier-slice theorem**:

$$[Rf]\hat{}(\theta, \gamma) = \hat{f}(\gamma \cos\theta, \gamma \sin\theta).$$

- ET Radon data can be numerically transformed into 2D Fourier samples on a polar grid. From a computational perspective, these are non-uniform discrete Fourier transform (NDFT) samples.
- Treating projections as NDFT data has been used in recent CS-ET work. Our approach uses non-transformed Radon domain data.

1. Introduction
2. Radon transforms and compressed sensing
3. Sparsity across application domains
4. Experimental results

Compressed sensing background

- Compressed sensing: Assume a signal (vector) $f : \mathbb{R}^D \to \mathbb{R}$, a set of M **measurement vectors** $\{\varphi_m\} \subseteq \mathbb{R}^D$, and a **representation frame** $\{\psi_n\}_{n=1}^N \subseteq \mathbb{R}^D$.
- Stack measurements in columns as measurement matrix $\Phi \in \mathbb{R}^{D\times M}$ and frame elements as representation matrix $\Psi \in \mathbb{R}^{D\times N}$.
- *A priori* signal assumption: f is s-sparse in Ψ: $||\Psi^T f||_0 \leq s$. (Analytic sparsity)
- Most existing CS results focus on orthonormal basis or tight frame Ψ for which $f = \Psi\Psi^T f$.

Compressed sensing background

- Goal: Given measurements $b = \Phi^T f$, efficiently recover f even if $M < N$ as:

$$f^* = \arg\min_{g \in \mathbb{R}^D} ||\Psi^T g||_1 \text{ such that } b = \Phi^T g. \tag{3}$$

- The feasibility of this approach depends on the structure of $\Theta \triangleq \Phi^T \Psi$.

Restricted isometry property

- Isometry constant δ_k: $k = 1, 2, \ldots$. The smallest nonnegative number such that

$$(1 - \delta_k)||x||_2^2 \leq ||\Theta x||_2^2 \leq (1 + \delta_k)||x||_2^2$$

for all k-sparse $x \in \mathbb{R}^N$.

- Theorem (Candes): If $\delta_{2s} < \sqrt{2} - 1$ given the previous hypotheses, (3) recovers f exactly.
- RIP bounds are difficult to verify directly. Estimates can be made by analyzing off-diagonal entries of $\Theta^T \Theta$.

CS for tomography

- Each sample $Rf(\theta_i, s_j)$ corresponds to a measurement vector $\varphi_{ij} \in \mathbb{R}^D$ stacked in measurement matrix Φ.
- Common choices of Ψ: Identity matrix, wavelet synthesis matrix, discrete cosine transform synthesis matrix.
- In ET, also common to let $\Psi^T = TV$ the total variation operator.
- For a 2D discrete image f,

$$TV f \triangleq \sqrt{\Delta_x^+ f + \Delta_y^+ f}$$

for forward finite $x-$ and $y-$differences Δ^+.

Theoretical challenges

- There is little theory in place for recovering f from (3) given nonlinear sparsifying transforms (e.g. TV).
- ET measurement matrices Φ are deterministic, do not satisfy RIP for useful (k, δ_k) values.
- Simple measurement variation: choose measurement angles $\{\theta_i\}$ randomly in some range.
- Still not RIP, empirically this performs worse than uniformly-spaced angle choices.

Radon RIP, random vs. uniform sampling images.

Non-RIP CS

- Nevertheless, empirical results are good.
- Question: Why does this work with non-RIP measurements? An open, practical problem for applying CS to many physical measurement situations.
- Thought: Are there additional *a priori* assumptions about signal structure that can be exploited for physical imaging?
- e.g. if Θ is (k, δ_k) RIP for some nice subset of k-sparse signals?

Additional challenges

- Equation (3) can be related to the regularized least-squares problem

$$f^* = \arg\min_{g \in \mathbb{R}^D} ||\Phi^T g - b||_2^2 + \lambda ||\Psi^T g||_1,$$

  for some weight parameter λ.

- This formulation allows for the use of multiple regularizers simultaneously; useful in practice but on shaky ground in CS theory.

- We used identity, DB8 wavelet and TV regularizers with three weight parameters

- Difficult to get good *a priori* estimates of optimal weight values.

1 Introduction

2 Radon transforms and compressed sensing

3 Sparsity across application domains

4 Experimental results

Image complexity across applications

- Sparse signal models rely on accurate prior knowledge about object structure.
- The statistical image properties which influence the choice of sparsity model correlate with imaging application domain.

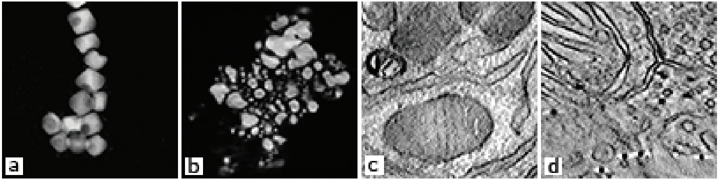

Figure: (a) Iron oxide nanoparticles, (Saghi et al., 2011). (b) Gallium-palladium nanoparticles, (Leary et al., 2013). (c) Renal cell section. (d) Retinal cell section.

Image complexity across applications

- Nanoparticle images - high-contrast features, piecewise-constant ("cartoon-like") intensities.
- Feature spatial scale may be large compared to the image's smallest-resolved spatial scale.
- Biological images - Features at varying contrasts and multiple spatial scales.
- Textural content due to noise, variations in embedding media, and structural features at or near highest resolution.

Image complexity across applications

- Image "complexity" is difficult to fully characterize but reflected in the sparsity/compressibility of the data.
- Nanoparticle images may be highly sparse in common sparsity models - identity sparsity, TV sparsity, wavelet sparsity.
- Biological images may be less sparse in all of these domains, hindering the efficacy of undersampled recovery.
- These observations are consistent with results in our work and the work of other groups on CS-ET in materials and biological sciences.

Compressibility image

Image complexity across applications

- The advantages of CS reconstruction come at the price of data-dependence.
- This fact and its implications bear careful explanation for non-mathematical practitioners.
- A comprehensive understanding of which sparsity models are appropriate for different image types would require an enormous organizational effort by the microscopy community.

1 Introduction

2 Radon transforms and compressed sensing

3 Sparsity across application domains

4 Experimental results

Numerical techniques

- The full equation our CS-ET algorithm minimizes is

$$f^* = \underset{g \in \mathbb{R}^D}{\arg\min} ||\Phi^T g - b||_2^2 + \lambda_1 ||g||_1 + \lambda_2 ||TVg||_1 + \lambda_3 ||Wg||_1 \tag{4}$$

  for each 2D slice of the tomogram, for some choice of regularization weights λ_i.

- 1024 2D slices, each 1024×256 (maybe thinner).
- This remains difficult to solve quickly on modern computational hardware.

The split-Bregman algorithm

- The split-Bregman algorithm for convex optimization solves problems with multiple ℓ^1 and ℓ^2 norm terms efficiently.
- Two-step iterative scheme that decouples the ℓ^1 and ℓ^2 minimizations in (4).
- ℓ^2 minimization can be solved by conjugate gradients (or better when possible), ℓ^1 by a fast shrinkage routine.
- This and naive parallelization (MATLAB's parfor routine) drops CS-ET reconstruction time on the new NWC workstation to under 30 minutes for the pancreatic cell tomogram.

split-Bregman phantom animation.

Experimental results

- For phantoms with the nanoparticle statistical properties, CS-ET recovery is markedly better than alternative methods.
- For biological tomograms, CS-ET matches or exceeds alternative methods, but by a smaller margin.
- Still demonstrates the feasibility of undersampled recovery, which is evidently of interest for some tomography applications.

Phantom + bio reconstruction comparison images

Future work - CS-ET

- The application of CS recovery algorithms to deterministic, non-RIP sensing problems suggests the need for new theoretical developments.
- Practically, there remain challenges for packaging CS-ET techniques for non-mathematical practitioners.
- Nontrivial choices for sparsity models, regularization parameters, number of Bregman iterations which may be data-dependent.
- Collaboration with NIBIB is ongoing for optimized numerical implementations for greater speed/use on their computing clusters.

Future work - Sparse inpainting

- Additionally for tomography, these results could be combined with sparse inpainting techniques to alleviate missing wedge artifacts.
- Missing wedge - Mechanical limitations force the range of $\{\theta_i\}$ samples to be smaller than $[-90°, 90°]$. Causes characteristic artifacts.
- Ariel and Ben are working with Wojtek to solve this problem.

Works cited

R Leary, Z Saghi, P Midgley, and D Holland. Compressed sensing electron tomography. Ultramicroscopy, 2013.

Z Saghi, D Holland, R Leary, A Falqui, G Bertoni, A Sederman, L Gladden, and P Midgley. Three-dimensional morphology of iron oxide nanoparticles with reactive concave surfaces. a compressed sensing-electron tomography (cs-et) approach. Nano letters, 11(11):4666–4673, 2011.